Accurate 3-D Position and Orientation Method for Indoor Mobile Robot Navigation Based on Photoelectric Scanning

Zhe Huang, Jigui Zhu, Linghui Yang, Bin Xue, Jun Wu, and Ziyue Zhao

Abstract—Position and orientation of indoor mobile robots must be obtained real timely during operation in structured industrial environment, so as to ensure the security and efficiency of cargo transportation and assembly precision. But for such a large-scale space, only 2-D coordinates and heading angle of the mobile robot can be measured with a relatively low precision in current major methods. This paper presents a novel method for 3-D position and orientation measurement of indoor mobile robot. In this method, a rotary-laser transmitter is utilized, which is mounted on the indoor mobile robot measuring the scanning angles relative to photoelectric artificial landmarks and obtaining its own 3-D space location information. The landmarks whose coordinates in navigation frame should be precalibrated are distributed at the most appropriate positions of the structured industrial environment. On the basis of that, an algorithm of multiangle intersection was established and in-depth discussed to solve transmitter's spatial position and orientation. Experimental results show that, in an 8 m × 6 m × 2.5 m working volume, transmitter's position, and orientation measurement accuracy of proposed method were higher than 3.8 mm and 0.104°, respectively. It demonstrates that the proposed method is reliable and flexible for indoor mobile robot navigation tasks and the measurement accuracy can be further improved by increasing layout density of landmarks.

Index Terms—3-D, large-scale space, measurement, navigation, orientation, position.

I. INTRODUCTION

INDOOR mobile robot is widely used in industrial applications such as cargo handling in vacuum cleaner platform [1], automated manufacture [2], large aerospace structures assembly [3], and so on. Accurate position and orientation data of the mobile robot platform are a basis of subsequent precise motion control and path planning in navigation process. In general, the position and orientation measurement methods for indoor mobile robot can be divided into two categories: 1) dead reckon and 2) absolute locating [4]. Dead reckon methods such as measurement

Z. Huang, J. Zhu, L. Yang, B. Xue, and Z. Zhao are with Tianjin University, Tianjin 300072, China (e-mail: jiguizhu@tju.edu.cn).

J. Wu is with the Civil Aviation University of China, Tianjin 300300, China.

Color versions of one or more of the figures in this paper are available online at http://ieeexplore.ieee.org.

Digital Object Identifier 10.1109/TIM.2015.2415031

by inertial measurement unit [5] or odometer [6] need neither external information nor radiate information outward, it can provide locating service for mobile robot independently, covertly, and continuously [7]. However, the measurement errors of dead reckon method are accumulated over time and this feature limits its application in navigation field. Thus, the data acquisition of mobile robots' position and orientation relies more on absolute locating methods.

Many research attentions about absolute locating methods have been received and as a result, significant advances have been made on this front. Among them, many methods based on landmarks have been provided for indoor mobile robot navigation applications such as vision [8], [9], ultrasonic [10]–[12], and other wireless positioning techniques [13]. However, the traditional and existing methods mostly suffer the limitations of low accuracy, low data-updating rate, and the multipath effect. Simultaneously, most of them cannot provide 3-D position and orientation service, which is tough to meet the requirements of modern indoor mobile robot navigation.

In recent decades, photoelectric measurement technology has developed rapidly and has been successfully demonstrated to serve in industrial environments. Based on this principle, intensive research efforts have been conducted and several alternative methods and devices have been proposed. The laser tracker is an off-the-shelf device, which is extensively applied in large-scale applications with flexibility, real-time 3-D coordinate measurement, and excellent accuracy. However, it is hard to be applied to indoor mobile robot navigation due to the lack of the ability to detect multiple targets simultaneously and does not allow for visibility restriction during the measurement; The vision with charge-coupled device sensors is a noncontact sensing method in which it is possible to obtain the necessary input information for computing the dynamic parameters of a moving object without disturbing the system. Although it is relatively cost effective, it could not provide 360° direction measurement and does not fit a changing background. It is also hard to identify the object's dynamics only based on the vision sensors [14]. The laser radar developed in [15] and [16] is a kind of popular positioning device. It scans its surroundings 2-D with a radial field of vision using infrared laser beams. It has been extensively applied in indoor mobile robots in industrial structured environment with its flexibility, real-time measurement, and low cost. However,

TABLE I
POSITION ACCURACY COMPARISON OF DIFFERENT DYNAMIC MEASUREMENT SYSTEMS

Category	Type	Company	Accuracy
Laser Tracker	AT901-LR	Leica	$\pm15\mu m+6\mu m/m$
Visual Dynamic Measurement System	V-STARS/D5	GSI	$14\mu m+14\mu m/m$
Indoor GPS	iSpace Dynamic Tracking Kit	Nikon	$0.3mm+10\mu m/m$
Laser Ladar	Nav300	SICK	$\pm15mm$

in some scenarios such as the high-precision assembly and docking procedure of large parts of the aircraft [17], the laser radar is unable to obtain the position and orientation of the mobile platform simultaneously and difficult to achieve a high accuracy with alto frequency. Table I shows the position accuracy comparison of some different dynamic measurement systems [18]–[21].

In this paper, aiming at the indoor mobile robot location problem in navigation process, a novel 3-D position and orientation measurement method based on photoelectric scanning principle was presented. This method is implemented by a rotary-laser transmitter mounted on the mobile robot and several photoelectric receivers as landmark distributed at the fixed positions. When the indoor mobile robot moves in the structured environment with the transmitter's measuring unit rotating in a fixed speed, scanning angles of the receivers relative to the transmitter are obtained by the system. If the laser planes can detect enough receivers, the 3-D coordinates and orientation angles of the transmitter can be calculated. By this method, the robot can see 360° around itself without limitation and the landmark receivers can be arranged at the position which has a good sight to the transmitter. In addition, since the communication is one way and all the process of signal perception are in the receiver side, navigation system does not need to deal with reflection signals, which is different from laser radar in principle and suppresses the multipath effect [22] in a certain extent. Therefore, the proposed method is considered as a faster, easier, and more efficient solution for indoor mobile robot's position and orientation measurement.

This paper is organized as follows. Section II describes the system composition and the working principle, including the obtaining method of scanning angles and the basic measurement model of the transmitter. Section III presents the mathematical solving method of the position and orientation, including the optimization calculation method and analysis of the initial iteration value. In Section IV, based on a precision linear guide and multitooth indexing table, experiments were performed to verify the repeatability and accuracy of the proposed method. Finally, in Section V, the conclusion and a brief overview of future improvements are presented.

II. PRINCIPLE OF MEASUREMENT

A. System Composition and Working Principle

As shown in Fig. 1, the system is composed of the following parts: the rotary-laser transmitter [23], the photoelectric
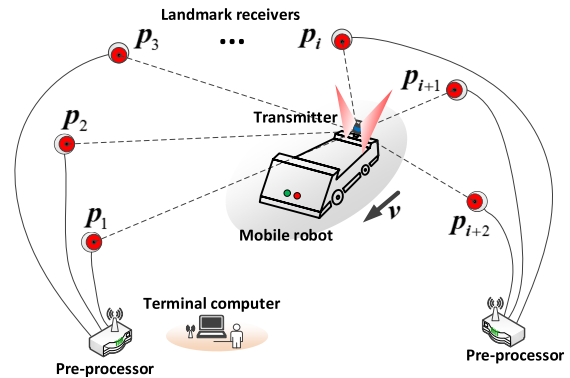

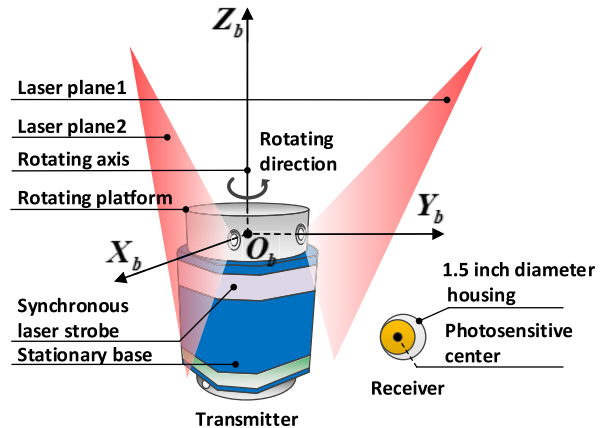Fig. 1. Position and orientation measurement system for indoor mobile robot.

Fig. 2. Schematic of the transmitter and landmark receiver.

receivers as landmark, the signal preprocessor, and the terminal computer.

Fig. 2 gives a schematic about the structure of transmitters and receivers of the transmitter and receiver. The transmitter mainly consists of a stationary base and the rotor. During the measurement process, the rotor keeps rotating and emitting optical signals to 360° direction space which can be captured by the receivers. After receivers receive these signals, the preprocessors analysis these signals and transmit the processing results to the terminal computer for final calculation. With the rotating head of the transmitter spinning at a predefined speed of approximately $60 \pi \, rad/s$ in anticlockwise direction, the transmitter generates three laser signals that provide plenty of optical messages for measurement. They are two nonparallel planar laser beams and a cyclical omni-directional laser strobe.
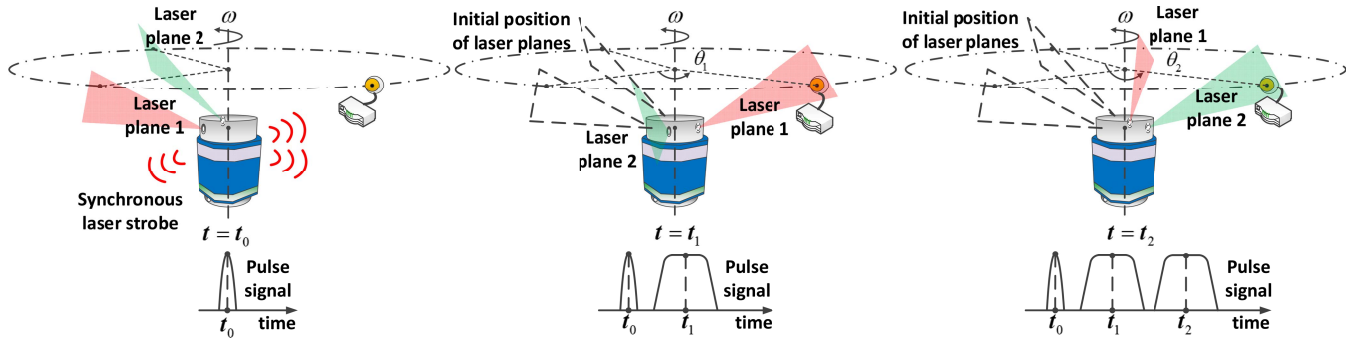
Fig. 3. Schematics of the scanning angle measurement at different times.

The two nonparallel planar laser beams are with different tilt angles rotating around the shaft in uniform motion. Simultaneously, the transmitter sends synchronous laser strobe as marks to scan in the measurement space when it rotates to a predefined position of every cycle.

The photoelectric receiver is made into a spherical component, with radius of 1.5 in for convenience when comparing the accuracy with the laser tracker. It can capture all of the three optical signals from the transmitter by its inside p-i-n diode and its internal circuits make sure the signals are adequately amplified and filtered. Then, the signals having been photo-electrically converted are sent to the signal preprocessor. As an important part of solution, the signal preprocessor with high-precision timing unit identifies different kind of electrical signals by pulsewidth and records the time interval between different laser planes and the synchronized laser strobes. The schematics are shown in Fig. 3.

Thus, this location method is based on precise scanning angle measurement that is different from laser radar in principle [24]. Assuming that the moment when the receiver capture the synchronized laser signal is t_0 and that when it captures the two scanning signals are t_1 and t_2, respectively, as the rotating speed is a constant value ω, then the scanning angle θ_1 of laser plane 1 from the initial position to the position when it passes through the receiver can be expressed as

$$\theta_1 = \omega \cdot (t_1 - t_0). \tag{1}$$

In the same way, to laser plane 2

$$\theta_2 = \omega \cdot (t_2 - t_0). \tag{2}$$

As can be observed from (1) and (2), the measurement accuracy of the scanning angle completely depends on the rotating speed and the timing moments. The control system built-in the transmitter has the ability to maintain a constant rotating speed and the preprocessor also keeps providing precision timing services. Thus, in the premise of achieving the same accuracy and comparing with other angle measuring methods [21]–[25], this method does not rely on the high-precision encoder and getting rid of the cumbersome calibration process, which makes our transmitter more cost effective and easy to be manufactured. In addition, by the
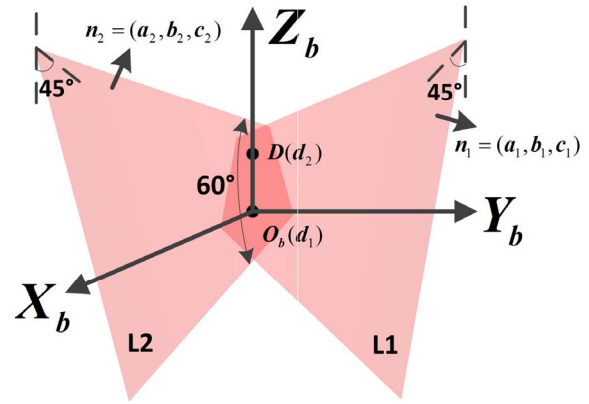

Fig. 4. Mathematical model of the double-plane constraint.

means of increasing the optical power of the laser module, the measurement range can be expanded to meet the actual demand in large spatial navigation task.

What is more, as the frequency of the synchronous laser strobe reflects the rotating speed of the transmitter directly, if more than two transmitters keep working simultaneously, they could be identified by the receiving and signal processing parts according to their different synchronous laser strobe frequencies. This feature makes both the landmark receivers and the transmitters expandable in quantity and endow this system the ability to support multiple tasks.

B. Basic Measurement Model of the Transmitter

As described in Section II-A, the scanning angles of the transmitter's rotary-laser planes can be obtained by a receiver. For position and orientation measurement of the transmitter fixed on the mobile robot, combined with several receivers as landmarks distributed at the fixed positions, the plane constraints based on the measurement model were introduced.

As shown in Fig. 4, the body coordinate frame of the mobile robot $O_b - X_b Y_b Z_b$ on the transmitter was established which is defined as follows: Z_b-axis is defined as the rotation axis. The intersection point between laser plane 1 in the initial position and the rotation axis is regarded as the original point. Through the original point, the plane vertical to Z_b-axis is defined as $X_b O_b Y_b$ plane and the intersection line of plane $X_b O_b Y_b$ and laser plane 1 in initial position is X_b-axis. Naturally, Y_b-axis is

determined by the right hand rule. When the rotor head is at the initial position, the two laser plane equations can be written as

$$\begin{cases} a_1 x + b_1 y + c_1 z + d_1 = 0 \\ a_2 x + b_2 y + c_2 z + d_2 = 0 \end{cases} \quad (3)$$

where $[a_1 \; b_1 \; c_1 \; d_1]^T$ and $[a_2 \; b_2 \; c_2 \; d_2]^T$ are precalibrated coefficients of laser planes 1 and 2, respectively. When the rotator head has rotated θ_m degrees from the initial position, the laser planes pass through the receiver and the following equations are established:

$$\begin{bmatrix} a_1(\theta_m) \\ b_1(\theta_m) \\ c_1(\theta_m) \\ d_1(\theta_m) \end{bmatrix} = \begin{bmatrix} R(\theta_m) & 0 \\ 0 & 1 \end{bmatrix} \cdot \begin{bmatrix} a_m \\ b_m \\ c_m \\ d_m \end{bmatrix}; \quad (m \in (1,2)) \quad (4)$$

where $R(\theta_m)$ is the rotation matrix around Z-axis. According to the space rigid body transformation theory [26], as there is no rotary motion along X-axis and Y-axis, the rotation matrix with the rotation angle θ_m can be written as

$$\begin{aligned} &R(\theta_m) \\ &= \begin{bmatrix} 1 & 0 & 0 \\ 0 & 1 & 0 \\ 0 & 0 & 1 \end{bmatrix} \cdot \begin{bmatrix} 1 & 0 & 0 \\ 0 & 1 & 0 \\ 0 & 0 & 1 \end{bmatrix} \cdot \begin{bmatrix} \cos\theta_m & -\sin\theta_m & 0 \\ \sin\theta_m & \cos\theta_m & 0 \\ 0 & 0 & 1 \end{bmatrix}. \quad (5) \end{aligned}$$

Therefore, the measuring model of single transmitter–receiver pair is based on the double-plane constraint as mentioned above. As the navigation frame can be set anywhere as global frame according to users' needs, if the transmitter detects multiple landmarks whose coordinates in the navigation frame are predefined, it is able to calculate the position and orientation of the indoor mobile robot by an efficient and fast algorithm.

III. POSITION AND ORIENTATION MEASURING ALGORITHM

A. Three-Landmarks Point Position and Orientation Calculation Method

According to the navigation coordinate frame $O - X_n Y_n Z_n$ and the transmitter body frame $O_b - X_b Y_b Z_b$ defined in Section II-B, the relationship of the same point P_i between the two different coordinate frames can be expressed as follows:

$$P_i^n = \begin{bmatrix} C_b^n & T_b^n \end{bmatrix} \cdot P_i^b \quad (6)$$

where

P_i^n the coordinate of the ith landmark in navigation frame;

P_i^b the coordinate of the ith landmark in transmitter body frame;

C_b^n the orientation transformation matrix from the transmitter body frame to the navigation frame;

T_b^n the translation matrix from the transmitter body coordinate frame to the navigation frame.

If the coordinates of at least three corresponding points in two different frames were known, the relationship between the two frames could be obtained, including the orientation transformation matrix C_b^n and the translation matrix T_b^n. As shown above, the coordinates of the receivers in the navigation frame and transmitter body frame are represented as $P_i^n = [x_i^n \; y_i^n \; z_i^n]$ and $P_i^b = [x_i^b \; y_i^b \; z_i^b]$, respectively. For obtaining the C_b^n, the following vectors are defined:

$$\begin{cases} \overrightarrow{P_1 P_2} = P_2 - P_1 \\ \overrightarrow{P_2 P_3} = P_3 - P_2 \\ Q = \overrightarrow{P_1 P_2} \times \overrightarrow{P_2 P_3}. \end{cases} \quad (7)$$

Substituting the different coordinate vectors into the conversion equations (6), and according to (7), they could be expressed as

$$\begin{cases} \overrightarrow{P_1 P_2}^n = C_b^n \cdot \overrightarrow{P_1 P_2}^b \\ \overrightarrow{P_2 P_3}^n = C_b^n \cdot \overrightarrow{P_2 P_3}^b \\ Q^n = C_b^n \cdot Q^b. \end{cases} \quad (8)$$

Assuming that

$$C_b^n = [R_1 \; R_2 \; R_3]^T = \begin{bmatrix} r_1 & r_2 & r_3 \\ r_4 & r_5 & r_6 \\ r_7 & r_8 & r_9 \end{bmatrix}. \quad (9)$$

By the x component of the three corresponding equations in (8), the vector $[r_1 \; r_2 \; r_3]$ can be obtained by solving the following linear equation set as:

$$\begin{cases} (\overrightarrow{P_1 P_2})_x^n = r_1 \cdot (\overrightarrow{P_1 P_2})_x^b + r_2 \cdot (\overrightarrow{P_1 P_2})_y^b + r_3 \cdot (\overrightarrow{P_1 P_2})_z^b \\ (\overrightarrow{P_2 P_3})_x^n = r_1 \cdot (\overrightarrow{P_2 P_3})_x^b + r_2 \cdot (\overrightarrow{P_2 P_3})_y^b + r_3 \cdot (\overrightarrow{P_2 P_3})_z^b \\ (Q)_x^g = r_1 \cdot (Q)_x^b + r_2 \cdot (Q)_y^b + r_3 \cdot (Q)_z^b. \end{cases} \quad (10)$$

Similarly, R_2 could be solved by y component. Since the coordinate system is orthogonal, R_3 could be obtained by cross multiplication of R_1 and R_2 as

$$R_3 = R_1 \times R_2. \quad (11)$$

If the orientation transformation matrix C_b^n has been determined, the three orientation angles of the transmitter are determined naturally which is represented as yaw (ψ), pitch (θ), and roll (γ). The relationship between the three orientation angles and the orientation transformation matrix C_b^n is shown as

$$\psi = \arctan\left(\frac{C_b^n(1,2)}{C_b^n(2,2)}\right)$$

$$\theta = \arcsin\left(C_b^n(3,2)\right)$$

$$\gamma = \arctan\left(-\frac{C_b^n(3,1)}{C_b^n(3,3)}\right). \quad (12)$$

Then, the translation matrix T_b^n can be obtained easily by averaging the three pairs of corresponding point vectors

$$T_b^n = \frac{\left(P_1^n + P_2^n + P_3^n - C_b^n \cdot P_1^b - C_b^n \cdot P_2^b - C_b^n \cdot P_3^b\right)}{3}. \quad (13)$$

B. Multilandmarks Position and Orientation Calculation Method

If the transmitter detects more than three receivers, the problem of determining the conversion matrix $[C_b^n \quad T_b^n]$ by multiple pairs of corresponding points can be converted to the least squares problem. Thus, the objective function is defined

$$\min F = \sum_{i=1}^{N} \left\| P_i^n - [C_b^n \quad T_b^n] \cdot P_i^b \right\|^2 \tag{14}$$

wherein $P_i^n = [x_i^n \ y_i^n \ z_i^n \ 1]$ and $P_i^b = [x_i^b \ y_i^b \ z_i^b \ 1]$ are the homogeneous coordinate representation of P_i^n and P_i^b, respectively. In (14), solving $[C_b^n \quad T_b^n]$ is a linear calculation process which needs at least four pairs of corresponding vectors and can be determined by the following formula:

$$[C_b^n \quad T_b^n] = G \cdot S^{-1} \tag{15}$$

where

$$G = \begin{bmatrix} P_1^n & P_2^n & P_3^n & P_4^n \\ 1 & 1 & 1 & 1 \end{bmatrix} \tag{16}$$

$$S = \begin{bmatrix} P_1^b & P_2^b & P_3^b & P_4^b \\ 1 & 1 & 1 & 1 \end{bmatrix}. \tag{17}$$

The necessary and sufficient condition for the existence of the solution $[C_b^n \quad T_b^n]$ is $|S| \neq 0$ which illustrates that the four points in space cannot be coplanar.

Based on the discussion above, if the number of the corresponding point is more than four, the calculation accuracy could be improved theoretically and the solutions can be obtained by least-squares linear regression [27]

$$[C_b^n \quad T_b^n] = G \cdot S^T \cdot (S \cdot S^T)^{-1} \tag{18}$$

where

$$G = \begin{bmatrix} P_1^n & P_2^n & \cdots & P_i^n \\ 1 & 1 & \cdots & 1 \end{bmatrix} \tag{19}$$

$$S = \begin{bmatrix} P_1^b & P_2^b & \cdots & P_i^b \\ 1 & 1 & \cdots & 1 \end{bmatrix}. \tag{20}$$

i represents the number of corresponding points and $i > 4$. However, the solutions obtained by (18) are not the optimal ones to determine the correspondence between two coordinate frames, for C_b^n does not satisfy the orthogonal constraints. Thus, the following least squares problem with orthogonal constraints is introduced:

$$\begin{cases} \min F = \sum_{i=1}^{N} \left\| P_i^n - [C_b^n \quad T_b^n] \cdot P_i^b \right\|^2 \\ R^T R - I = 0. \end{cases} \tag{21}$$

constructing the orthogonal constraint as the following functions:

$$\begin{cases} h_1 = r_1^2 + r_4^2 + r_7^2 - 1 \\ h_2 = r_2^2 + r_5^2 + r_8^2 - 1 \\ h_3 = r_3^2 + r_6^2 + r_9^2 - 1 \\ h_4 = r_1 r_2 + r_4 r_5 + r_7 r_8 \\ h_5 = r_1 r_3 + r_4 r_6 + r_7 r_9 \\ h_6 = r_2 r_3 + r_5 r_6 + r_8 r_9. \end{cases} \tag{22}$$

Converting the constrained optimal objective function into unconstrained optimal objective function by penalty function method

$$\min F = \sum_{i=1}^{N} \left\| P_i^n - [C_b^n \quad T_b^n] \cdot P_i^b \right\|^2 + M \sum_{i=1}^{6} h_i^2 \tag{23}$$

where M is the penalty factor to control the error magnitude for solving C_b^n.

As described above, to measure the position and orientation of a moving object needs numbers of landmark control points whose coordinates are known in two coordinate frames. The coordinates of the landmarks in the navigation coordinate frame are calibrated accurately before the navigation task, thus to obtain the position and orientation angles of the transmitter, calculating the coordinates of the landmarks in the transmitter body frame is needed.

Assuming there are a number of laser planes swept over the landmark receivers whose coordinates as unknown in transmitter body frame are denoted by $[x_i^b \ y_i^b \ z_i^b]^T$, based on the double-plane constraints discussed in Section II, when the laser planes pass through the receivers, the following equations are listed:

$$\begin{cases} F_{1i} = a_{1i}(\theta_{1i}) \cdot x_i + b_{1i}(\theta_{1i}) \cdot x_i + c_{1i}(\theta_{1i}) \cdot x_i + d_{1i} = 0 \\ F_{2i} = a_{2i}(\theta_{2i}) \cdot x_i + b_{2i}(\theta_{2i}) \cdot x_i + c_{2i}(\theta_{2i}) \cdot x_i + d_{2i} = 0 \\ f_m = L_{ij} - \left\| P_i - P_j \right\| = 0. \end{cases} \tag{24}$$

Among them, L_{ij} is the distance between any two different landmarks. Assuming that there are i landmark receivers receiving the laser signals from the transmitter, the unknown quantities P_i which are to be determined include $3i$ parameters as $[x_i \ y_i \ z_i]^T$. From (3), each transmitter–receiver pair gives two plane-constraint equations and among the receivers, any two receivers give one distance-constraint equation. Thus, at least plane-constraint equations and $(1/2)i(i-1)$ distance-constraint equations can be established totally as (23). For obtaining the solutions, it must be ensured that the condition that $(1/2)i(i-1) + 2i \geq 3i$ is satisfied which is equivalent to $i \geq 3$. Based on the discussion above and (24), the coordinates of corresponding landmarks can be calculated by minimizing the following function:

$$\min E = \sum_{i=1}^{N} \left(F_{1i}^2 + F_{2i}^2 \right) + M \sum_{m=1}^{\frac{1}{2}N(N-1)} f_j^2. \tag{25}$$

Similar with (23), N represents the number of the landmark receivers to be detected. M is the penalty factor and both of them are nonlinear minimization problem, which can be solved by the Levenberg–Marquardt algorithm [28].

C. Analysis of the Initial Iteration Value

Levenberg–Marquardt is a kind of least squares fitting method whose solution is obtained by iterative method. When using this method, a good initial value must be provided and it should be as much as possible in the vicinity of the true value, otherwise the result may converge to the other extreme points or even cannot converge. From what have been
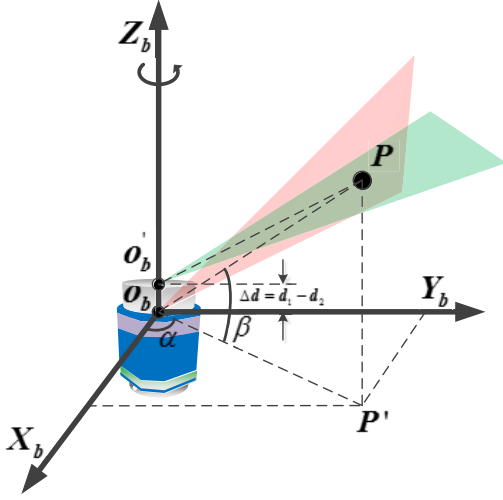
Fig. 5.   Approximate measurement of the horizontal and vertical angles.

discussed above, solving the coordinate of the landmarks in the transmitter body frame is the premise of estimating the position and orientation of the transmitter. Thus, to obtain the initial iteration value, this paper utilizes the feature that the transmitter has the ability of measuring the approximate horizontal and vertical angles of the landmark. The method is shown as follows.

As mentioned, one of the laser plane coefficients $d_i (i = 1, 2)$ is the intercept along the Z-axis in the transmitter coordinate frame, which is guaranteed by assembly adjustment and therefore relatively small. According to the definition of coordinate frame $O_b - X_b Y_b Z_b$, d_1 should be 0. Thus, the formula $\Delta d = d_1 - d_2 \approx 0$ is established, which illustrates that the two laser planes intersect at the origin point approximately. When the two laser planes pass through the landmark P_i one by one, respectively, at different times, they intersect to form a straight line from the origin of the transmitter body coordinate frame to P_i as shown in Fig. 5. Assuming the direction vector of this straight line is denoted as l_i, it can be expressed as

$$l_i = n_{i1} \times n_{i2} = (r_{ix} \ r_{iy} \ r_{iz}) \tag{26}$$

where n_{i1} and n_{i2} are two normal vectors of the transmitter laser planes. And the horizontal angle α and vertical angle β can be represented as:

$$\begin{cases} \alpha = \arctan\left(\dfrac{r_{iy}}{r_{ix}}\right) \\ \beta = \arctan\left(\dfrac{r_{iz}}{\sqrt{r_{ix}^2 + r_{iy}^2}}\right). \end{cases} \tag{27}$$

If the approximate distances between the landmarks and the transmitter are known which is denoted as d_i, the approximate coordinate $\tilde{P}_i$ as initial iteration can be obtained by the following expressions:

$$\tilde{P}_i = d_i \cdot [\cos\beta \cdot \cos\alpha \quad \cos\beta \cdot \sin\alpha \quad \sin\beta]^T. \tag{28}$$

As the most basic case that the transmitter can detect only three landmark receivers, d_i can be calculated by solving the following equations:

$$\cos(\theta_{ij}) = \frac{d_i^2 + d_j^2 - L_{ij}^2}{2 d_i d_j}; \quad (i, j \in (1, 2, 3) \cap (i \neq j)) \tag{29}$$

where $\theta_{ij} = \arccos((l_i \cdot l_j)/(|l_i| \cdot |l_j|))$ represents the angle between any two lines; L_{ij} is the distance between different landmarks which is precalibrated.

Obviously, there are three unknowns in (29), which has certain solutions theoretically. However, this calculation method presents multiple roots which cannot be distinguished directly [8]. Yet as the mobile robot moving in a structural industrial field, there is some prior knowledge of the working environment such as the differences of distance between different landmarks to the transmitter and the dynamic states at previous times. The error solution can eliminated by this information which is described in detail below.

The working process of the mobile robot can be divided into two main phases: 1) initialization phase and 2) running phase. In the initialization phase, the transmitter on the mobile robot usually remains stationary at a fixed position and this moment is regarded as t_0. Based on the prior knowledge in the space, the approximate distances at this moment from the transmitter to different landmarks can be known in advance or easily obtained by other ranging instruments such as portable laser rangefinder or ultrasonic rangefinder [29]. As the different roots of the distances mentioned above vary greatly with each other, the true solution can be easily selected by this method. In the running phase, as the mobile robot keeps moving in continuous mode, the output results of adjacent moments have strong correlation with each other. To obtain a sufficient number of measurement dates, the sampling period T should be set quite short. Simultaneously, to ensure operating safely in the industrial environment, the mobile robot does not need to move quickly. According to the formula $\Delta s = v \cdot T$, as the mobile robot's moving velocity does not exceed 200 mm/s generally and the sampling period of the signal preprocessor is not slower than 0.1 s, logically its moving distance between two adjacent measurement results updating moments must be less than 0.02 m. Since this distance is relatively short, the true coordinates calculated from the previous moment can be used as the initial iteration value for the calculation in next moment. Thus, the determining process of the initial value in the two phases can be summarized as (30), and Fig. 6 gives a schematic illustration of the discussion above

$$\begin{cases} \tilde{P}_i^t = d_i \cdot [\cos\beta \cdot \cos\alpha \quad \cos\beta \cdot \sin\alpha \quad \sin\beta]^T \\ \tilde{P}_i^t = P_i^{t-1}; \quad ((t \geq nT), n \geq 1). \end{cases} \tag{30}$$

IV. Experimental Results

A. Setup of the Verification Platform

To adequately verify the proposed algorithm, two independent experiments were designed to test the accuracy of position and orientation measurement. The transmitter and the landmark receiver are shown in Fig. 7.

As shown in Fig. 8, the measurement system includes one transmitter, six Receivers, and one signal preprocessor, which were designed and manufactured by Tianjin University, China.
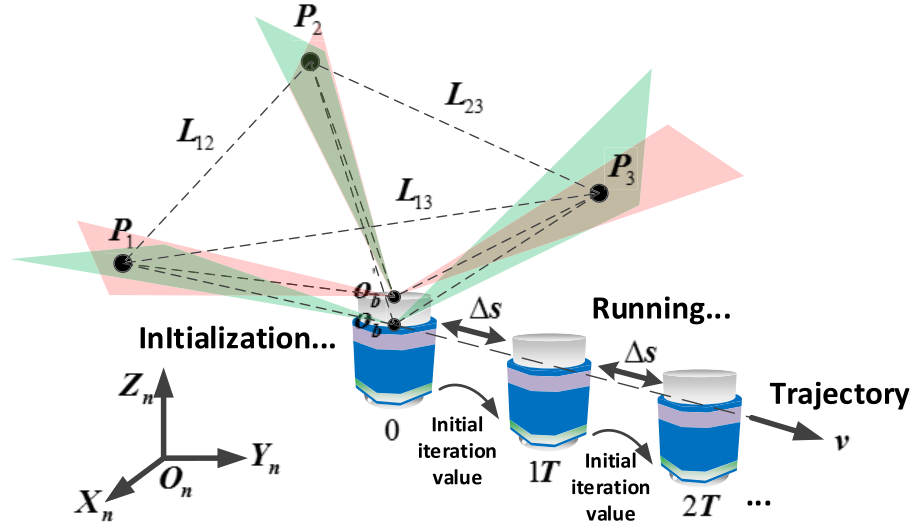
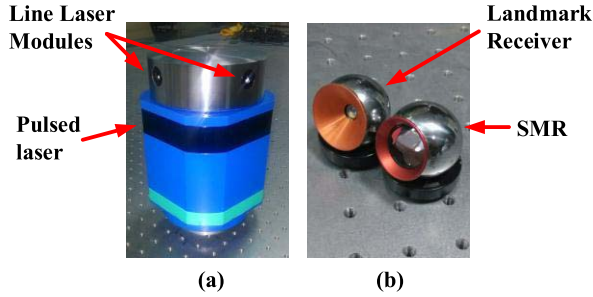Fig. 6. Approximate solution of the landmark coordinates.

Fig. 7. Transmitter landmark receiver and SMR in experiment. (a) Transmitter. (b) Receiver and SMR.

The accuracy of transmitter's scanning angle measurement is within $\pm 2''$. By means of calibration, the plane coefficients of the transmitter's laser planes were precalibrated as

$$\begin{bmatrix} a_1 \\ b_1 \\ c_1 \\ d_1 \end{bmatrix} = \begin{bmatrix} 0 \\ -0.79452674 \\ 0.60722917 \\ 0 \end{bmatrix}, \quad \begin{bmatrix} a_2 \\ b_2 \\ c_2 \\ d_2 \end{bmatrix} = \begin{bmatrix} -0.81989998 \\ 0.00766409 \\ 0.57245549 \\ 2.74583370 \end{bmatrix}. \quad (31)$$

The angular velocity of transmitter's rotating head was set as $\omega = 60 \ \pi \, \text{rad/s}$. To verify the accuracy of position and orientation measurement, a linear guide with moving stage and a multitooth indexing table were also introduced.

For measuring the position and orientation of the transmitter, numbers of receivers were put at the positions whose coordinates were fixed in the experimental field. According to the algorithm presented above, more than three noncollinear receivers should be detected. Without loss of generality and as a basic condition, six landmark receivers were used as landmark and their coordinate calibration in navigation frame was accomplished by the Leica AT901-LR laser tracker. The calibration result is listed in Table II, and the instruments in this verification platform are arranged, as shown

TABLE II
COORDINATES OF THE RECEIVERS IN NAVIGATION
FRAME (UNIT: MILLIMETERS)

Point ID	X coordinate x_p	Y coordinate y_p	Z coordinate z_p
Landmark 1	6610.839	129.12	952.74
Landmark 2	4719.442	1728.299	2153.04
Landmark 3	4723.476	2703.185	2150.54
Landmark 4	4724.948	4671.676	2144.13
Landmark 5	4719.113	5831.355	2150.47
Landmark 6	6604.87	6478.24	1601.7

in Fig. 8. It is important to note that as the receiver and the processor identify different transmitters by their rotating speed, to ensure their anti-interference performance and prevent the misrecognition phenomenon, we put the transmitter B in the experimental site and regard it as the sources of interference for simulating the multitasking navigation scenarios. Under such conditions, transmitter A would be tested and the experiments were carried out as follows.

B. Verification of the Position Measurement Accuracy

Comparative experiments of position measurement in three spatial directions were performed to verify the feasibility and the accuracy of the proposed method, which is shown in Fig. 9. The distance between the three landmark receivers and the transmitter is about 5 m in 8 m × 6 m × 2.5 m volume and the navigation coordinate frame was set up on the laser tracker. One spherically mounted reflector (SMR) on the transmitter was tracked, which is convenient to compare the measuring result with the laser tracker as a standard. During this experiment, a precision linear guide with
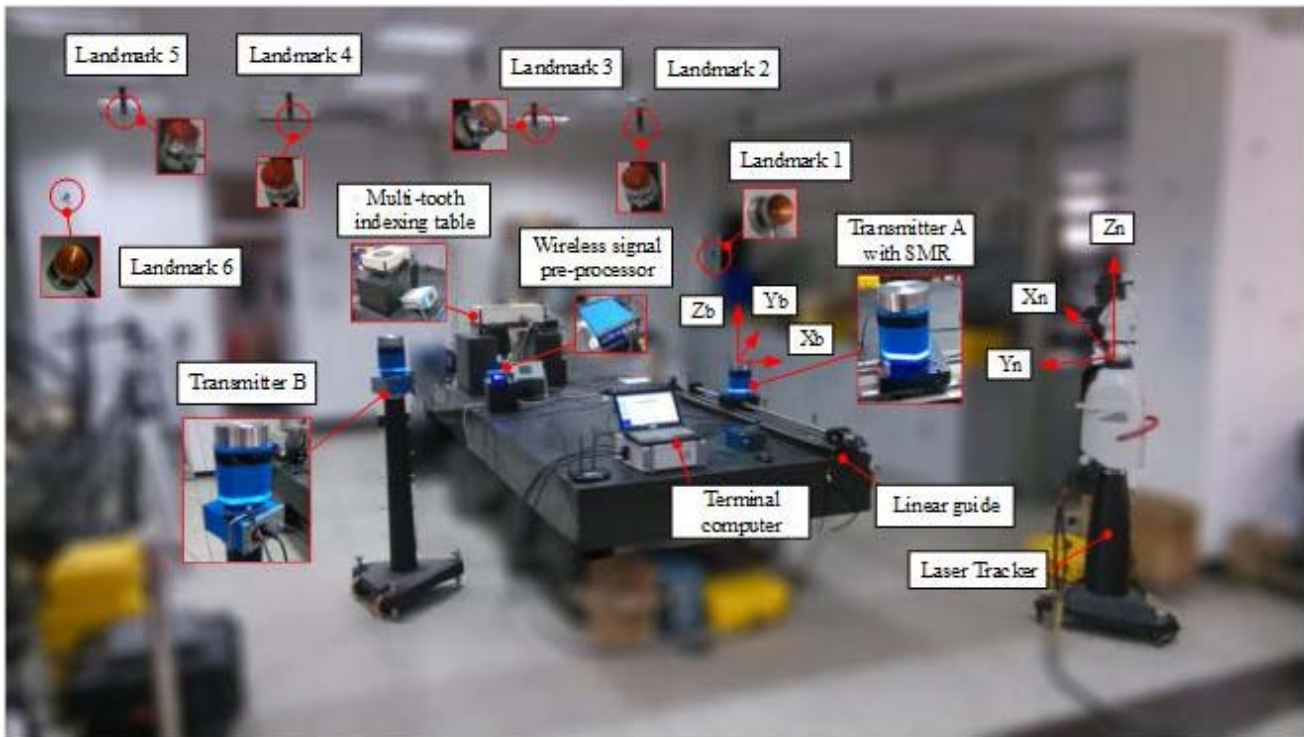
Fig. 8. Experiment platform of the position and orientation measurement system.
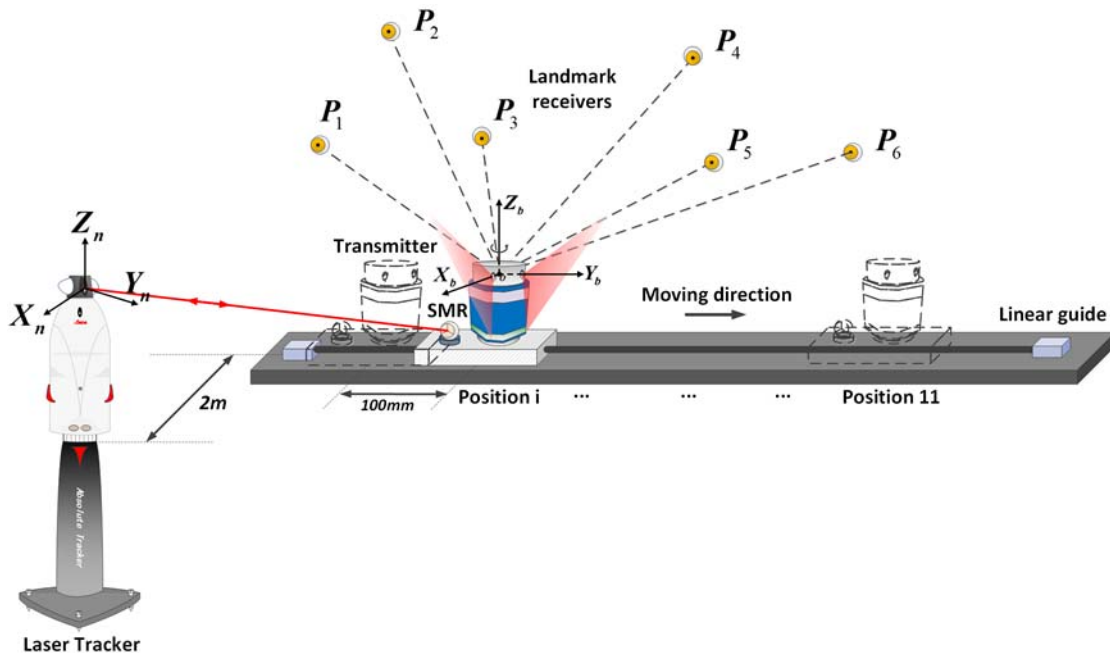

Fig. 9. Schematic of comparison experiment of position measurement.

movement stage which simulates the movement of mobile robot was used to keep the transmitter trajectory a straight line in two directions (X_n and Y_n directions, respectively). In each direction, the transmitter on the movement stage was moved along the guide with the same distance to numbers of successive positions and obtained the current coordinates through the proposed algorithm.

As an evaluation basis of coordinate measurement accuracy, repeatability experiment is necessary [30]. To verify the measurement stability, the coordinates of the transmitter at a fixed position were measured 500 times with the interval of 1 s repeatedly and recorded the coordinate measuring result. The comparison results are shown in Table III. The standard deviations of the coordinate measurement in the three direc-

TABLE III

REPEATABILITY EVALUATION OF POSITION MEASUREMENT (UNIT: MILLIMETERS)

	Max	Min	Average	Standard deviation
x	1889.767	1889.580	1889.662	0.050
y	2653.957	2652.299	2653.154	0.606
z	-982.65	-983.125	-983.005	0.091
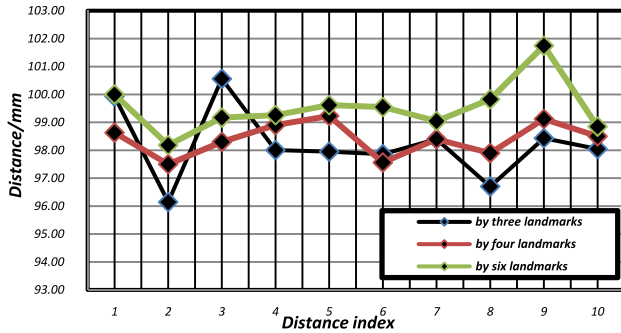
Fig. 10.　Moving distance of the transmitter in X_n-direction.

Fig. 11.　Moving distance of the transmitter in Y_n-direction.

TABLE IV

REPEATABILITY EVALUATION OF ORIENTATION MEASUREMENT (UNIT: DEGREE)

	Max	Min	Average	Standard deviation
YAW	-24.791	-24.830	-24.817	0.0076
PITCH	-1.900	-1.921	-1.907	0.0040
ROW	-0.366	-0.373	-0.371	0.0015

tions were 0.050, 0.606, and 0.091 mm, respectively. And the deviations between the maximum and minimum value were 0.187, 1.658, and 0.475 mm, respectively. From the results above, it could be seen that the error in Y_n-direction is much larger than that in X_n and Z_n directions, this is attributed to the fact that the proposed method is essentially based on the measurement of scanning angles, which provides a weak constraint in Y_b-direction and makes the accuracy in this direction more sensitive to that of the scanning angle measurement [30]. Then, the measurement error propagated through the coordinate transformation from the transmitter frame to the navigation frame.

With the transmitter and the SMR fixed together as a rigid body on the linear guide, their moving distance error was inspected simultaneously. In the premise that the repeatability of position measurement was in a relatively low range, if the method proposed before can reach a high-positioning accuracy, their moving distance should be the same as far as possible. The motion stage moved along the X_n-direction approximate every 100 mm from the starting position and each movement distance was recorded by the laser tracker. The comparison of distance measurement in the X_n-direction was also performed in the same way. As the guide is less than 1.5-m long, each movement distance was measured 10 times by three landmarks, four landmarks, and six landmarks, respectively, and the comparison results are shown in Figs. 10 and 11.

From Figs. 10 and 11, it is clear that taking the laser tracker as a standard in experiment, by three-point coordinate calculation algorithm, the maximum distance errors are 3.8 and 2.4 mm, respectively, along the X_n-direction and the Y_n-direction. The ones calculated by four-point and six-point coordinate conversion algorithm are relatively further smaller, which shows that using more landmarks could improve the positioning accuracy in a certain extent. Since it is hard to ensure that the center position of the landmark receiver be
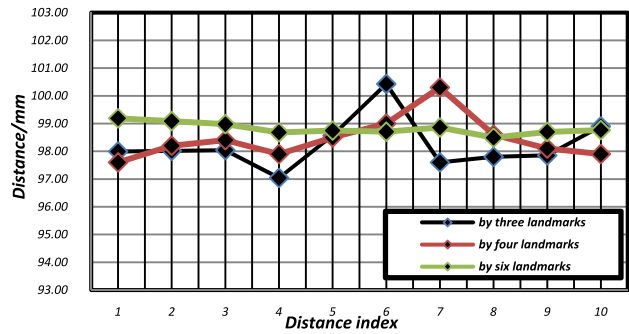
absolutely at the same position with the one of the SMR, the final measuring error in this magnitude is quite acceptable. In summary, this result could demonstrate that the proposed method is effective which can be used in the mobile robot positioning tasks with high accuracy.

C. Verification of the Orientation Measurement Accuracy

For orientation measurement, the proposed method was validated by measuring the Euler angles relative to the navigation frame and comparing the results with that measured by the laser tracker. The schematic is shown in Fig. 12.

As the position measuring verification experiment, the repeatability of orientation measurement with the proposed method should also be evaluated. The three Euler angles along with the axis of the navigation frame were measured and calculated 500 times repeatedly, and the results are shown in Table III. As shown in Table IV, the standard deviations of the orientation angles are 0.0076°, 0.004°, and 0.0015°, respectively. It can be seen from the results that the angle measuring repeatability errors in three directions were all quite small. Although yaw error is relatively larger, this magnitude of orientation accuracy can be guaranteed in dozens of arc seconds [31].

According to the same evaluation method with position measurement, it is hard to obtain the true absolute orientation angles of the transmitter directly. However, as most mobile robots working on the ground, the heading angle along with the rotation axis of the transmitter is significant whose accuracy needs to be guaranteed adequately. The pitch and roll of the transmitter are relatively small during its smoothly running process. Thus, the orientation measurement accuracy was mainly inspected under the condition of changing the transmitter's heading angles by multitooth indexing table and compared the results with laser tracker.
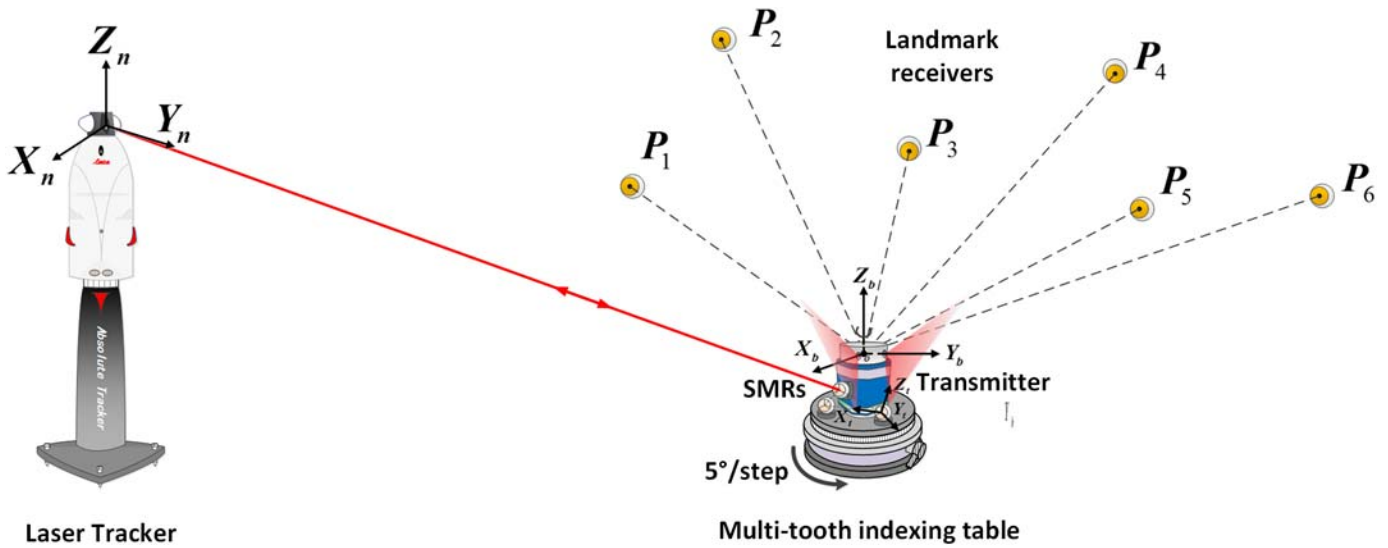
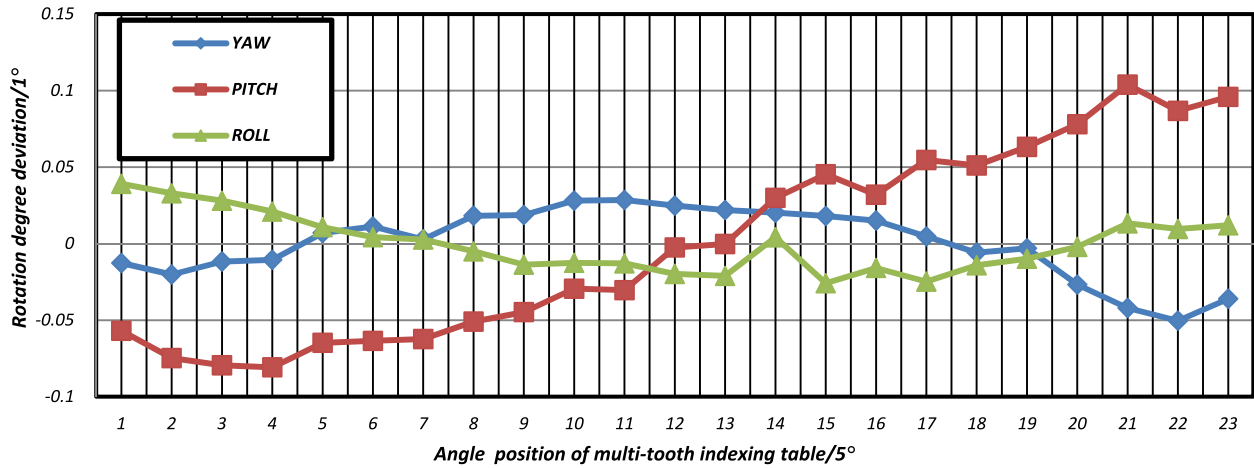Fig. 12.   Schematic of comparison experiment of orientation measurement.

Fig. 13.   Deviations of yaw, pitch, and roll.

The experiment is described as below: first, the transmitter was put on a multitooth indexing table whose angle repeatability accuracy is $0.6''$ for convenient rotation along with the transmitter's shaft which simulated the variation of the heading angle during mobile robot working. Three SMRs were attached to the transmitter body which can form a new coordinate frame $O_t - X_t Y_t Z_t$ by direct coordinate measurement using the laser tracker. The schematic is shown in Fig. 12. As the transmitter and the three SMRs fixed on its stationary base which constituted a rigid body, together with the table rotating different heading angles, the rotational relationship between the transmitter frame, and the custom coordinate frame should be determined and constant. The Euler angles measured by this verification method between $O_b - X_b Y_b Z_b$ and $O_t - X_t Y_t Z_t$ are shown in Fig. 13. In this figure, the X-axis represents each rotation step $(5°)$ of the multitooth indexing table, and the Y-axis represents the deviation of rotation angle whose resolution is $0.05°$. The maximum deviations of yaw, pitch, and roll were $0.029°$, $0.104°$, and $0.039°$, respectively. As can be observed in Fig. 13, the deviation of pitch presents drift

upward trend with the increase of angular positions and in contrast, the yaw and roll changed relatively smaller. However, no matter how obvious the drift trend measurement results will appear, the accuracy of our orientation measurement method fully meets the requirements of attitude monitoring during its working in real time [32].

V. CONCLUSION AND DISCUSSION

A new method with a relative high accuracy for measuring the position and orientation of a mobile robot in 3-D space has been proposed. This method utilizes a transmitter with two rotary laser planes mounted on the mobile robot and several photoelectric receivers as landmark distributed in the industrial environment. The measurement principle is expounded in detail, including the scanning angle measurement and the iterative solution algorithm based on multiplane constraint. The feasibility and accuracy of this position and orientation measurement method are verified by the laser tracker in comparison experiments. The results obviously demonstrate

the flexibility and superiority of this method to other location systems which satisfies most mobile robot navigation tasks.

In the field of position and orientation measurement of moving target, laser tracker is an ideal instrument with its excellent accuracy and dynamic performance. But compared with the method which was proposed in this paper, its high cost and single task work cause that it could not be widely used in the field of mobile robot navigation. In addition, in the applications in large scale space and multitasking measuring environment, our method depends on increasing the landmark receivers to expand the measurement volume that is different from the indoor GPS system and avoids the complicated global orientation process. Furthermore, the landmark receivers can be put anywhere according to the navigation tasks, this feature make the light blocking problem be weakened which is superior to other optical and photoelectric measurement methods.

For practical applications, as the method requires clear line of sight to be ensured between the transmitter and the receivers, the landmark receivers could be put at the most suitable locations that are influenced little by other obstructions. Also for avoiding the occlusion phenomenon as much as possible, large number of receivers could be laid, which reduces the possibility of robots into the blind. About other respects of the proposed method, some more digging and detailed efforts are needed such as the ways to increase the measurement range and frequency and make the volume of transmitter smaller. And how to improve the measurement stability and locating accuracy in pure dynamic state should also be further studied in coming days. In addition, as the experiment result shows that using more landmarks can improve the measurement accuracy to some extent, how to set their quantity and position distribution in industrial site is also a key issue. About the hardware design optimization of whole system, there still exist some shortcomings. For example, the wired connection between the landmark receivers and the signal processor is some cumbersome. However, it is still being tested in the experimental condition. In coming days, we will connect each part of the system wirelessly and make this method more suitable for practical application.

ACKNOWLEDGMENT

REFERENCES

[1] P. Jensfelt, H. I. Christensen, and G. Zunino, "Integrated systems for mapping and localization," in *Proc. IEEE/RSJ Int. Conf. Intell. Robots Syst.*, May 2002, pp. 5007–5012.

[2] W. Tan, "Modeling and control design of an AGV," in *Proc. 41st IEEE Conf. Decision Control*, vol. 1. Dec. 2002, pp. 904–909.

[3] L. Schulze and A. Wullner, "The approach of automated guided vehicle systems," in *Proc. IEEE Int. Conf. Service Oper. Logistics, Informat.*, Jun. 2006, pp. 522–527.

[4] C.-C. Tsai, "A localization system of a mobile robot by fusing dead-reckoning and ultrasonic measurements," in *Proc. IEEE Instrum. Meas. Technol. Conf.*, vol. 1. May 1998, pp. 144–149.

[5] J. Collin, O. Mezentsev, and G. Lachapelle, "Indoor positioning system using accelerometry and high accuracy heading sensors," in *Proc. ION GPS/GNSS Conf.*, 2003, pp. 9–12.

[6] R. Mautz and S. Tilch, "Survey of optical indoor positioning systems," in *Proc. Int. Conf. Indoor Positioning Indoor Navigat.*, Sep. 2011, pp. 1–7.

[7] A. Bergeron and N. Baddour, "Design and development of a low-cost multisensor inertial data acquisition system for sailing," *IEEE Trans. Instrum. Meas.*, vol. 63, no. 2, pp. 441–449, Feb. 2014.

[8] O. A. Yakimenko, I. I. Kaminer, W. J. Lentz, and P. A. Ghyzel, "Unmanned aircraft navigation for shipboard landing using infrared vision," *IEEE Trans. Aerosp. Electron. Syst.*, vol. 38, no. 4, pp. 1181–1200, Oct. 2002.

[9] N. Alt and E. Steinbach, "Navigation and manipulation planning using a visuo-haptic sensor on a mobile platform," *IEEE Trans. Instrum. Meas.*, vol. 63, no. 11, pp. 2570–2582, Nov. 2014.

[10] M. O. Khyam, M. J. Alam, A. J. Lambert, C. R. Benson, and M. R. Pickering, "High precision ultrasonic positioning using a robust optimization approach," in *Proc. 18th Int. Conf. Digit. Signal Process.*, Jul. 2013, pp. 1–6.

[11] M. McCarthy, P. Duff, H. L. Muller, and C. Randell, "Accessible ultrasonic positioning," *IEEE Pervasive Comput.*, vol. 5, no. 4, pp. 86–93, Oct./Dec. 2006.

[12] C. Medina, J. C. Segura, and A. de la Torre, "A synchronous TDMA ultrasonic TOF measurement system for low-power wireless sensor networks," *IEEE Trans. Instrum. Meas.*, vol. 62, no. 3, pp. 599–611, Mar. 2013.

[13] L. Hui, H. Darabi, P. Banerjee, and L. Jing, "Survey of wireless indoor positioning techniques and systems," *IEEE Trans. Syst., Man, Cybern. C, Appl. Rev.*, vol. 37, no. 6, pp. 1067–1080, Nov. 2007.

[14] G. N. DeSouza and A. C. Kak, "Vision for mobile robot navigation: A survey," *IEEE Trans. Pattern Anal. Mach. Intell.*, vol. 24, no. 2, pp. 237–267, Feb. 2002.

[15] V. Nguyen, A. Harati, and R. Siegwart, "A lightweight SLAM algorithm using orthogonal planes for indoor mobile robotics," in *Proc. IEEE/RSJ Int. Conf. Intell. Robots Syst.*, Oct./Nov. 2007, pp. 658–663.

[16] A. Hagemann, "NAV 200 SICK navigation," Jan. 2008, pp. 1–67. [Online]. Available: http://www.sick.com/

[17] S. Naing, "Feature based design for jigless assembly," Ph.D. dissertation, School Ind. Manuf. Sci., Cranfield Univ., Cranfield, U.K., 2004.

[18] SICK. (2013). *Laser Scanners NAV300-2232*. [Online]. Available: https://www.mysick.com/PDF/Create.aspx?ProductID=33788&Culture=en-US

[19] Geodetic Systems Inc. *V-STARS/D5*. [Online]. Available: http://www.geodetic.com/f.ashx/BROCHURES/D5-Brochure, accessed 2013.

[20] Nikon Metrology. (2013). *iSpace for Dynamic Tracking and Alignment: A 6 doF Measurement Solution for Guidance & Automation*. [Online]. Available: http://www.nikonmetrology.com/content/download/12362/251053/version/10/file/iSpace_Dynamic+tracking_EN.pdf

[21] *PCMM System Specifications Leica Absolute Tracker and Leica T-Products*, Hexagon Metrology, 2009.

[22] Q. Spencer, M. Rice, B. Jeffs, and M. Jensen, "A statistical model for angle of arrival in indoor multipath propagation," in *Proc. IEEE 47th Veh. Technol. Conf.*, May 1997, pp. 1415–1419.

[23] Z. Zhao, J. Zhu, B. Xue, and L. Yang, "Optimization for calibration of large-scale optical measurement positioning system by using spherical constraint," *J. Opt. Soc. Amer. A*, vol. 31, no. 7, pp. 1427–1435, 2014.

[24] M. U. de Haag, D. Venable, and M. Smearcheck, "Use of 3D laser radar for navigation of unmanned aerial and ground vehicles in urban and indoor environments," *Proc. SPIE*, vol. 6550, pp. 65500C-1–65500C-12, May 2007.

[25] Y. Matsuzoe, N. Tsuji, T. Nakayama, K. Fujita, and T. Yoshizawa, "High-performance absolute rotary encoder using multitrack and M-code," *Opt. Eng.*, vol. 42, no. 1, pp. 124–131, 2003.

[26] J. C. Juang and G.-S. Huang, "Development of GPS-based attitude determination algorithms," *IEEE Trans. Aerosp. Electron. Syst.*, vol. 33, no. 3, pp. 968–976, Jul. 1997.

[27] P. Geladi and B. R. Kowalski, "Partial least-squares regression: A tutorial," *Anal. Chim. Acta*, vol. 185, pp. 1–17, Jul. 1986.

[28] J. J. Moré, "The Levenberg–Marquardt algorithm: Implementation and theory," in *Numerical Analysis*. Berlin, Germany: Springer-Verlag, 1978, pp. 105–116.

[29] J. Wu, J. Zhu, L. Yang, M. Shen, B. Xue, and Z. Liu, "A highly accurate ultrasonic ranging method based on onset extraction and phase shift detection," *Measurement*, vol. 47, pp. 433–441, Jan. 2014.

[30] Z. Liu, J. Zhu, L. Yang, H. Liu, J. Wu, and B. Xue, "A single-station multi-tasking 3D coordinate measurement method for large-scale metrology based on rotary-laser scanning," *Meas. Sci. Technol.*, vol. 24, no. 10, p. 105004, 2013.

[31] J. J. Leonard and H. F. Durrant-Whyte, "Mobile robot localization by tracking geometric beacons," *IEEE Trans. Robot. Autom.*, vol. 7, no. 3, pp. 376–382, Jun. 1991.

[32] S. J. Julier and J. K. Uhlmann, "A counter example to the theory of simultaneous localization and map building," in *Proc. IEEE Int. Conf. Robot. Autom.*, May 2001, pp. 4238–4243.
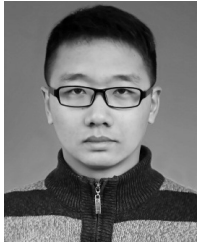
Zhe Huang was born in Shenyang, China, in 1989. He received the M.S. degree in precision measuring technology and instruments from Tianjin University, Tianjin, China, in 2013, where he is currently pursuing the Ph.D. degree in precision measuring technology and instruments.

His current research interests include photoelectric precision measuring and mobile robot navigation.

Jigui Zhu received the B.S. and M.S. degrees from the National University of Defense Science and Technology, Changsha, China, in 1991 and 1994, respectively, and the Ph.D. degree from Tianjin University, Tianjin, China, in 1997.

He is currently a Professor with the State Key Laboratory of Precision Measurement Technology and Instruments, Tianjin University. His current research interests include laser and photoelectric measuring technology, such as industrial online measurement and large-scale precision metrology.

Linghui Yang received the Ph.D. degree from Tianjin University, Tianjin, China, in 2010.

He is currently a Lecturer with the State Key Laboratory of Precision Measurement Technology and Instruments, Tianjin University. His current research interests include large-scale coordinate measurement and photoelectric measuring technology.

Bin Xue received the M.S. degree in precision measuring technology and instruments from Tianjin University, Tianjin, China, in 2011, where he is currently pursuing the Ph.D. degree in precision measuring technology and instruments.

His current research interests include photoelectric precision measuring and large-scale precision metrology.

Jun Wu received the bachelor's degree in measuring and controlling technology and instrument, in 2009, and the Ph.D. degree in instrument science and technology from Tianjin University, Tianjin, China, in 2014.

He is currently a University Lecturer with the College of Aeronautical Automation, Civil Aviation University of China, Tianjin. His current research interests include large-scale metrology, digital photogrammetry, and robotics.

Ziyue Zhao received the M.S. degree in precision measuring technology and instruments from Tianjin University, Tianjin, China, in 2012, where he is currently pursuing the Ph.D. degree in precision measuring technology and instruments.

His current research interests include photoelectric precision measuring and large-scale precision metrology.